tures as high as 300°K, and there is no obvious reason why these thresholds should not also be evident for CdTe if they are really present. Second, this analysis leaves unexplained the lowest segments of the absorption which are drawn in to fit the data below segment (a) in each case. These segments cannot be fitted into the theoretical framework already described. Last, the indirect band gaps and threshold energies used in the calculation are only 10 to 15×10^{-3} eV smaller than the energy for the peak absorption by the direct excitons. In this part of the spectrum, less than one LO phonon away from the exciton center, phonon-assisted absorption by direct excitons is expected and, as shown in the following paper, all of the observed intrinsic absorption can be accounted for by this process. Thus it is concluded that no major fraction of the intrinsic absorption observed in CdTe below the direct-exciton peak can be plausibly understood as indirect interband or indirect exciton absorption, and there is no definite evidence that any of the absorption arises from such processes.

ACKNOWLEDGMENTS

Special thanks are due to Dr. M. R. Lorenz and Dr. R. E. Halsted for supplying the zone-refined CdTe ingots without which this study could not have been undertaken. Thanks are also due to Miss G. P. Lloyd and Miss E. L. Kreiger for assistance in obtaining and analyzing the transmission data. The helpful advice and comments of Dr. B. Segall are also acknowledged with thanks.

PHYSICAL REVIEW VOLUME 150, NUMBER 2 14 OCTOBER 1966

Optical Absorption Edge in CdTe: Theoretical*

B. SEGALL
General Electric Research and Development Center, Schenectady, New York
(Received 9 May 1966)

Optical absorption in the "edge region" (i.e., for photon energies just below the first exciton peak) due to the creation of direct excitons with the simultaneous absorption of one and two longitudinal optical phonons is calculated by perturbation theory for Wannier excitons formed from the conduction and valence bands around $\mathbf{k}=0$. It is shown that the contributions from the $n>1$ exciton bands, neglected in earlier calculations, are quite important and are required for a quantitative study. The results quantitatively account for the magnitude and for the temperature and energy dependences of the absorption coefficient observed in CdTe using a (average) hole mass of $0.4m$, where m is the free-electron mass. These results strongly support the assignment to CdTe of a "direct" minimum band gap at $\mathbf{k}=0$, contrary to a number of recent contentions (also based on absorption measurements) that the material is "indirect." It is noted that the agreement between the calculated results (including a rough correction for level broadening) and the data extends up to the temperature range at which the absorption coefficient begins to exhibit Urbach's-rule behavior. It is argued from this fact that the mechanism employed in these calculations, as opposed to others recently considered, underlies Urbach's rule in, at least, the compound semiconductors.

I. INTRODUCTION

THE temperature and energy dependence of the optical absorption of CdTe has been repeatedly measured in the neighborhood of the lowest-energy absorption edge[1] and the analyses of these data have suggested that this semiconductor has an "indirect" minimum band gap. The results of an investigation of a related phenomenon, the photovoltaic effect,[2] have been interpreted as favoring this assignment. Furthermore, a calculation of the valence band structure has supported this picture.[3,4] However, the results of the measurements of the intrinsic absorption edge in CdTe by Marple, which are presented in the previous paper[5] (hereafter referred to as I) differ in some significant respects from the earlier data. In addition, it was shown that the data in I could not be understood in terms of a reasonable indirect band gap model.

In this paper we start with the opposite assumption about the lowest band gap in CdTe, that is, that it is direct.[6] Furthermore, on the basis of the study of the

* This work was supported in part by the Aerospace Research Laboratories, Office of Aerospace Research, U. S. Air Force.

[1] P. W. Davis and T. S. Shilliday, Phys. Rev. **118**, 1020 (1960); C. Konak, Phys. Status Solidi **3**, 1274 (1963); W. Giriat, Acta Phys. Polon. **24**, 191 (1963).

[2] W. G. Spitzer and C. A. Mead, J. Phys. Chem. Solids **25**, 443 (1964).

[3] M. Cardona, J. Phys. Chem. Solids **24**, 1543 (1963).

[4] Professor Cardona has kindly brought to our attention the discovery of an algebraic error in Ref. 3 [see M. Cardona, J. Phys. Chem. Solids **26**, 1351 (1965)]. When the correction is remedied, the calculations yield a positive heavy hole mass.

[5] D. T. F. Marple, preceding paper, Phys. Rev. **150**, 728 (1966), hereafter referred to as I.

[6] The fact that this assignment is quite reasonable for CdTe, and indeed for all the II–VI semiconducting compounds, is discussed by B. Segall, in *Physics and Chemistry of II–VI Semiconducting Compounds*, edited by M. Aven and J. S. Prener (North-Holland Publishing Company, Amsterdam, to be published), Chap. 1.

electrical transport properties[7] and cyclotron resonance[8] in n-type material, we take this direct gap to be at $\mathbf{k}=0$. The absorption mechanism that we consider for photon energies below the lowest exciton line is the creation of a "direct" exciton with the simultaneous absorption of a longitudinal optical (LO) phonon. This process has been employed earlier to explain the absorption edge in the wurtzite crystals CdS[9] and ZnO.[10] We will show that this mechanism, with the assumption that the valence and conduction band extrema are at $\mathbf{k}=0$, leads to an absorption coefficient which is in good quantitative agreement with the measured values for CdTe.

Recent measurements and analyses along the lines discussed below indicate that the phonon-assisted direct exciton process also accounts for all the intrinsic edge-region absorption in ZnSe[11] and ZnTe.[12,13] These results appear to conflict with views of Aten *et al.*,[14] who measured the transmission in ZnTe and concluded that the material is "indirect" and with Cardona,[3,4] who calculated a negative hole mass at $\mathbf{k}=0$ for ZnSe. Furthermore, on the basis of all relevant available data it has been suggested that all of the II–VI compounds have direct $\mathbf{k}=0$ band gaps.[13,6] If this suggestion is borne out, the absorption edges in all these materials will be determined by the above mechanism. Similar conclusions probably apply to the III–V family, the majority of which appear to be "direct" semiconductors,[15] although the specifically "excitonic" aspects will be somewhat reduced due to weaker exciton binding and oscillator strengths.

Phonon-assisted direct transitions in the absorption edge region were first considered by Dumke[16] in processes involving free electrons and holes, i.e., in the so-called band-to-band transitions. The calculations for CdS[9] and ZnO[10] were similar except that the two-particle electronic states involved were taken to be discrete exciton states. In these latter studies, the calculations were greatly simplified by the assumption that only the $n=1$ exciton state makes an important contribution to the sums over intermediate and final states. While it appears that the results thus obtained are qualitatively correct, it is not clear without further investigation what contribution is made by the full spectrum (both discrete and continuum) of excited states. In fact, it will be shown (Sec. II) by simple considerations that the contribution of higher excited states cannot be neglected on the basis of previously given arguments. A principal purpose of this paper is to determine to what extent the contributions of the higher exciton bands modify the simple "$n=1$ only" result (Sec. II).

We also calculate (Sec. III) the absorption coefficient for the process involving the annihilation of two LO phonons, which is important in the range of one to two LO phonon energies below the first exciton line and at moderately high temperatures. With the latter results we extend our considerations over reasonably wide energy and temperature ranges.

For many insulators it has been shown that at sufficiently high temperatures the absorption coefficient in the edge region obeys Urbach's rule,[17] i.e., $\alpha\sim\exp\{-(E_0-h\nu)/\gamma k_B T\}$. Recently, considerable attention has been given to the problem of understanding the origins of this simple result. Since the Urbach behavior pertains to the same portion of the spectrum that we are concerned with here, although perhaps at somewhat higher temperatures, the question naturally arises as to what connection, if any, it has to the mechanism discussed above. This question will be discussed in Sec. IV.

In Sec. V we evaluate the possibility that other electron-phonon couplings could lead to appreciable contributions to the absorption coefficient in the spectral range of interest.

II. THE ONE-PHONON PROCESS

In this section we will calculate the optical absorption coefficient for the process involving the creation of a direct exciton and the simultaneous annihilation of an LO phonon and a photon of energy $h\nu$. This process has a threshold at $h\nu=E_{x,1}-\hbar\omega_l$, where $E_{x,1}$ is the position of the $n=1$ exciton absorption peak and $\hbar\omega_l$ is the energy of an LO phonon at $\mathbf{q}\approx 0$. (Phonon creation does not enter because we restrict ourselves to $h\nu<E_{x,1}$.) To describe the unperturbed electron and hole (exciton) system we employ an "effective mass" Hamiltonian, H_x, with the electron-hole interaction taken to be $-e^2/\epsilon_s|r_e-r_h|$, where ϵ_s is the static dielectric constant. This approximate Hamiltonian determines the eigenvalues and eigenfunctions which modulate the valence- and conduction-band Bloch functions in the complete wave function for the state. The effective-mass approximation should be applicable for the semiconductors under consideration (certainly for CdTe, the material we consider in detail) because of the moderately high dielectric constants (~ 10) and low reduced effective masses ($\sim 0.1m$). A further approximation, that of

[7] B. Segall, M. R. Lorenz, and R. E. Halsted, Phys. Rev. **129**, 2471 (1963).
[8] K. K. Kanazawa and F. C. Brown, Phys. Rev. **135**, A1757 (1964).
[9] D. G. Thomas, J. J. Hopfield, and M. Power, Phys. Rev. **119**, 570 (1960).
[10] R. E. Dietz, J. J. Hopfield, and D. G. Thomas, J. Appl. Phys. Suppl. **32**, 2282 (1961).
[11] G. E. Hite, D. T. F. Marple, M. Aven, and B. Segall (to be published).
[12] D. T. F. Marple (to be published).
[13] B. Segall and D. T. F. Marple, in *Physics and Chemistry of II–VI Semiconducting Compounds*, edited by M. Aven and J. S. Prener (North-Holland Publishing Company, Amsterdam, to be published), Chap. 7.
[14] A. C. Aten, C. Z. Van Doorn, and A. T. Vink, in *Proceedings of the International Conference on Physics of Semiconductors, Exeter, 1962* (Institute of Physics and The Physical Society, London, 1963), p. 696.
[15] O. Madelung, *Physics of III–IV Compounds* (John Wiley & Sons, Inc., New York, 1964).
[16] W. P. Dumke, Phys. Rev. **108**, 1419 (1957).
[17] For example, see R. S. Knox, in *Solid State Physics*, edited by F. Seitz and D. Turnbull (Academic Press Inc., New York, 1963), Suppl. 5.

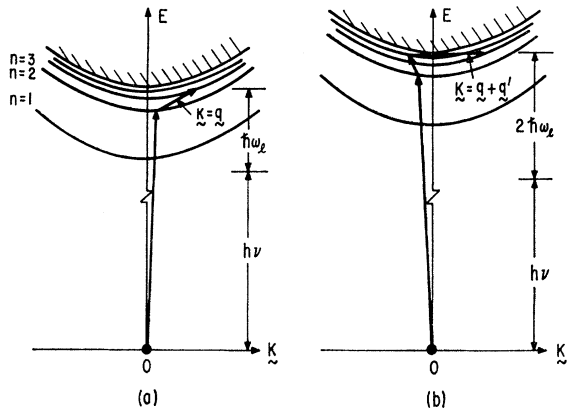

FIG. 1. Schematic representation of the one-phonon (a) and two-phonon (b) assisted "direct" exciton optical absorption processes. The dot at $E=0$ represents the ground state, the parabolas the discrete exciton bands, and the hatched area the continuous spectrum. The smaller arrows between the bands symbolize the "scattering" of the intermediate state excitons by the LO phonons.

representing the complex degenerate valence band by a simple spherical band characterized by a mass m_h, considerably simplifies the problem. Since the much lighter electron largely determines the exciton structure and, further, since the details of the valence band structure would not be expected to reflect themselves in an essential way in this process, this approximation should have no serious consequence. The parameter m_h is then some average over constants (the inverse masses A, B, and C)[18] describing the degenerate valence bands. The unperturbed exciton Hamiltonian is then

$$H_x=\frac{-\hbar^2}{2m_e}\nabla_{r_e}^2-\frac{\hbar^2}{2m_h}\nabla_{r_h}^2-\frac{e^2}{\epsilon_s r}$$
$$=\frac{-\hbar^2}{2M}\nabla_R^2-\frac{\hbar^2}{2\mu}\nabla_r^2-\frac{e^2}{\epsilon_s r}, \quad (1)$$

where $M=m_e+m_h$ and $\mu^{-1}=m_e^{-1}+m_h^{-1}$, $\mathbf{R}=M^{-1}(m_e\mathbf{r}_e+m_h\mathbf{r}_h)$, and $\mathbf{r}=\mathbf{r}_e-\mathbf{r}_h$. The energy spectrum is "hydrogenic,"

$$E_{xn}(\mathbf{K})-E_G=-B/n^2+\hbar^2\mathbf{K}^2/2M, \quad (2)$$

where the binding energy $B=\mathrm{Ry}\epsilon_s^{-2}(\mu/m)$ with $\mathrm{Ry}\equiv\mathrm{Rydberg}=13.6$ eV; $\mathbf{K}$ is the total exciton wave vector; and the integer n is the principal quantum number for the discrete states. For the continuum states, the internal energy is $\hbar^2\mathbf{k}^2/2\mu$, where $\hbar\mathbf{k}$ is the relative momentum. The eigenfunctions are

$$V^{-1/2}\exp(i\mathbf{K}\cdot\mathbf{R})\varphi_{\mathbf{n}}(\mathbf{r}), \quad (3)$$

with V the normalization volume and $\varphi_{\mathbf{n}}(\mathbf{r})\equiv\varphi_{nlm}(\mathbf{r})$ the standard hydrogen-atom wave functions (for the discrete and continuum states), with the exciton Bohr radius $a=a_0\epsilon_s(m/\mu)$, where a_0 is the atomic Bohr radius.[19,20]

The parts of the total Hamiltonian representing the unperturbed lattice vibrations and the electron-phonon coupling are

$$H_L+H_{eL}=\sum_{\mathbf{q},\sigma}\hbar\omega_\sigma(\mathbf{q})a_{\mathbf{q},\sigma}^*a_{\mathbf{q},\sigma}$$
$$+\sum_{\mathbf{q},\sigma,j}\{u_j(\mathbf{q})a_{\mathbf{q}\sigma}e^{i\mathbf{q}\cdot\mathbf{r}_j}+\mathrm{H.c.}\}, \quad (4)$$

where $j=e$ (electron) and h (hole), σ labels the mode, and $a_{\mathbf{q},\sigma}(a_{\mathbf{q},\sigma}^*)$ is the operator which annihilates (creates) a phonon of wave vector $\mathbf{q}$ and mode σ and H.c. denotes Hermitian conjugate. For the temperatures and $\mathbf{q}$ that we are concerned with, the most important coupling is that arising from the interaction of the electronic particles and the polarization associated with the LO vibrations, the so-called polar interaction (see Sec. V). For this case,

$$u_i(\mathbf{q})=(\pm)u(q)$$
$$=(\pm)i[e^2 2\pi\hbar\omega_l V^{-1}(\epsilon_\infty^{-1}-\epsilon_s^{-1})]^{1/2}q^{-1}, \quad (5)$$

where ϵ_∞ is the high-frequency dielectric constant and the different signs occur for the electron and hole. Since the optical branch is quite flat around $\mathbf{q}=0$ and only small momenta are important for weakly bound excitons, it is a good approximation to take $\omega(\mathbf{q})=$ constant. Finally, we must include the energy of the free radiation field H_R and electron-photon interaction term, which for the transition of interest is

$$H_{eR}=e(mc)^{-1}A(\mathbf{r}_e)\xi\cdot\mathbf{p}_e, \quad (6)$$

where $A(\mathbf{r}_e)$ is electromagnetic potential at $\mathbf{r}_e$ with polarization vector ξ, and $\mathbf{p}$ is the momentum operator for the electron. The total Hamiltonian H for the system is taken to be the sum of the unperturbed part H_0 and a perturbation H', with

$$H_0=H_x+H_L+H_R,$$
$$H'=H_{eR}+H_{eL}. \quad (7)$$

The process being considered is illustrated in Fig. 1(a), where the ground state of the crystal $|G\rangle$ is indicated by a dot at $E=0$ and the parabolas indicate the various exciton bands $E_{xn}(\mathbf{K})=E_{xn}+(\hbar^2/2M)\mathbf{K}^2$. In the first step of the process, which we treat by conventional perturbation theory, the exciton is created in band n with total momentum $\hbar\mathbf{K}\approx0$ (vertical selection rule) when the photon is annihilated. The exciton then undergoes a scattering to a state with $\mathbf{K}\neq0$ in the band n' with the absorption of a phonon of wave vector $\mathbf{q}$. The transition rate for the process is

$$w_{\mathbf{q}}^{(\mathbf{n}')}=2\pi/\hbar\left|\sum_{\mathbf{n}}\frac{\langle G|H_{eR}|\mathbf{n};0\rangle\langle\mathbf{n};0|H_{eL}|\mathbf{n}';q\rangle}{E_{xn}-h\nu}\right|^2$$
$$\times\delta(h\nu+\hbar\omega_l-E_{xn'}-\hbar^2q^2/2M). \quad (8)$$

[18] G. Dresselhaus, A. Kip, and C. Kittel, Phys. Rev. **98**, 368 (1955); E. O. Kane, J. Phys. Chem. Solids **1**, 249 (1957).

[19] G. Dresselhaus, J. Phys. Chem. Solids **1**, 14 (1956).

[20] R. J. Elliott, Phys. Rev. **108**, 1384 (1957).

Here, $\sum_n$ denotes the sum (and integral) over the complete hydrogenic spectrum including the discrete and continuous parts. The matrix elements are evaluated by making use of the usual separation of the rapidly and slowly varying parts of the exciton wave functions. As shown in the study of exciton line absorption,[20] the first matrix element can be written

$$em^{-1}[2\pi\hbar\eta(\boldsymbol{\kappa})/\epsilon'\omega]^{1/2}(\xi_\kappa\cdot\mathbf{P}_{vc})\varphi_{\mathrm{n}}(0), \tag{9}$$

where $\eta(\boldsymbol{\kappa})$ is the number of photons with wave vector $\boldsymbol{\kappa}$, ϵ' is the dielectric constant at $h\nu=E_{x1}$ with the contribution from the $n=1$ state omitted, and $\mathbf{P}_{vc}$ is the momentum matrix element connecting the $\mathbf{k}\approx 0$ valence- and conduction-band Bloch functions. To obtain (9) the k dependence of the band matrix element is neglected. Since $\varphi_{\mathrm{n}}(0)$ vanishes for $l\neq 0$, there are transitions only to the s exciton states in this approximation. Nonvanishing matrix elements (of H_{eR}) to the p, d, $\cdots$ exciton states, which arise from the part of the band matrix elements proportional to k, k^2, $\cdots$, are much smaller than those for the s exciton[20] and will be neglected below. Since the q's involved prove to be small [viz., $q\lesssim(1/30)(2\pi/a_{\mathrm{lattice}})$ for CdTe], the scattering matrix elements can be separated into rapidly and slowly varying parts, and can be expressed as

$$N(\hbar\omega)^{1/2}\delta_{\mathbf{q},\mathbf{K}}u(\mathbf{q})\int d^3r\ \varphi_{\mathrm{n}}^*(\mathbf{r})$$
$$\times[\exp(i\mathbf{q}\cdot\mathbf{r}m_e/M)-\exp(-i\mathbf{q}\cdot\mathbf{r}m_h/M)]\varphi_{\mathrm{n}'}(\mathbf{r})$$
$$=\delta_{\mathbf{q},\mathbf{K}}N(\hbar\omega)^{1/2}u(\mathbf{q})[\mathbf{n}|U(\mathbf{q})|\mathbf{n}'], \tag{10}$$

with $N(\hbar\omega)=(e^{\hbar\omega/kT}-1)^{-1}$. The reduced matrix element $[\mathbf{n}|U(\mathbf{q})|\mathbf{n}']$ is essentially the difference of two Fourier transforms of $\varphi_{\mathrm{n}}\varphi_{\mathrm{n}'}$, and its vanishing for $q\to 0$ and $\mathbf{n}'=\mathbf{n}$ reflects the over-all neutrality of the exciton.

To arrive at the absorption coefficient, we must sum over all permissible final-state exciton bands $\mathbf{n}'$ and all $\mathbf{K}=\mathbf{q}$, the latter introducing a density-of-states factor, and use the relation

$$\alpha=(\epsilon')^{1/2}[c\eta(\nu)]^{-1}\partial\eta/\partial t, \tag{11}$$

where $\eta(\nu)$ is the photon density in the range $(\nu,\ \nu+d\nu)$. Using $\partial\eta/\partial t=\sum_{\mathbf{q},n'}w_{\mathbf{q}}^{(n)}$, we obtain

$$\alpha(h\nu)=\alpha_0E_{x1}^2\pi a^3N(\hbar\omega_l)$$
$$\times\sum_{\mathbf{n}'}{}'\left|\sum_{n(l=0)}\frac{\varphi_{n,l=0}(0)[n,0|U(\mathbf{q})|\mathbf{n}']}{E_{xn}-h\nu}\right|^2_{\mathbf{q}=\mathbf{q}_{n'}}$$
$$\times E_{x1}^{1/2}(h\nu+\hbar\omega_l-E_{xn'})^{-1/2}, \tag{12}$$
$$\alpha_0=\frac{4\pi\beta_1}{(\epsilon')^{1/2}}\frac{e^2}{\hbar c}\frac{\hbar\omega_l}{4E_{x1}^{1/2}}\left(\frac{1}{\epsilon_\infty}-\frac{1}{\epsilon_s}\right)\left(\frac{2M}{\hbar^2}\right)^{1/2}.$$

The quantity $4\pi\beta_1$ represents the contribution to the polarizability from the $n=1$ excitons and is directly proportional to the oscillator strength per molecule for the $n=1$ line, $f_1[4\pi\beta_1(E_{x1}/\hbar)^2=4\pi e^2m^{-1}(\bar{N}/V)f_1$, where $\bar{N}/V$ is the number of molecules per unit volume]. As indicated, the matrix elements are to be evaluated at $q=q_{n'}$, where $q_{n'}$ is determined by conservation of energy and momentum;

$$\hbar^2\mathbf{q}_{n'}{}^2/2M=h\nu+\hbar\omega_l-E_{xn'}. \tag{13}$$

The prime on $\sum_{\mathbf{n}'}{}'$ indicates that the sum runs over only the accessible final bands, i.e., those for which $\mathbf{q}_n{}^2\geq 0$. The above result has already been given by Toyozawa[21] in his study of the exciton problem. By the use of damping theory, he has shown that the linewidths Γ_n and level shifts ΔE_{xn} enter in the expected manner, i.e., the energy denominators $E_{xn'}-h\nu$ are replaced by $E_{xn'}+\Delta E_{xn'}-h\nu+i\Gamma_{n'}$. We temporarily neglect these effects. The problem we address ourselves to is the evaluation of Eq. (12) to the required accuracy.

The simplest approximation, restricting the intermediate and final states to the $n=1$ band, leads to

$$\alpha_1(h\nu)=\alpha_0[E_{x1}/(E_{x1}-h\nu)]^2N(\hbar\omega_l)$$
$$\times\{[1+(p_h/2)^2]^{-2}-[1+(p_e/2)^2]^{-2}\}^2$$
$$\times E_{x1}^{1/2}(h\nu+\hbar\omega_l-E_{x1})^{-1/2}, \tag{14}$$

where $p_j=qam_j/M$ ($j=e$ or h). The quantity in the braces is the difference of the Fourier transforms of $|\varphi_{n=1}|^2$. Aside from a factor close to unity, $(m_h{}^2-m_e{}^2)\times(m_h{}^2+m_e{}^2)^{-1}$, this is the same expression as that given by Dietz *et al.*[10] The work of the remainder of the section is to consider the corrections to this expression. It is easy to see that (14) is a reasonable approximation when $\hbar\omega_l\ll B$. For, in that case, the relative smallness of the energy denominator for the $n=1$ band accentuates the contribution of that state to the sum over intermediate states, while energy conservation restricts the final states to that same band. Unfortunately, this simplifying condition does not apply for the semiconducting compounds of interest (in fact, generally $\hbar\omega_l>B$).

The previous arguments[9] to the effect that the $n>1$ intermediate states can be neglected because the oscillator strength drops off as n^{-3}, and that the continuum states can be ignored because of the large energy denominators which enter squared and the weakness of the scattering from these states to a bound state, are not as convincing as they first appear. First of all, since the square of the sum over intermediate states is involved, it is the ratio and not the square of the ratio of the various matrix elements and energy denominators that is relevant. The n-dependent factors in the intermediate state sum are principally $\varphi_n(0)<\varphi_n|$ which is n^{-3}. However, this fairly rapid dropoff is completely offset by the n^3 dependence of the density (in energy) of the discrete states, and the same effective weighting applies to the low-energy continuum states. It also turns out that when the normalization and density-of-states

[21] Y. Toyozawa, J. Phys. Chem. Solids **25**, 59 (1964); Y. Toyozawa, Progr. Theoret. Phys. (Kyoto) **20**, 53 (1958).

effects are accounted for, the appropriately "weighted" scattering matrix elements from lower continuum states are nearly equal to those from all but the lowest discrete states. While these arguments in themselves do not show that the $n>1$ bands make an important contribution, they do indicate that a more detailed study is required.

A. Intermediate States

We first consider the corrections due to the $n>1$ intermediate states, limiting the final states to $n=1$. These are the only corrections for $h\nu+\hbar\omega_l-E_{x1}<\frac{3}{4}B$, i.e., below the $n=2$ threshold. Also, for the conditions generally met in the compound semiconductors ($\hbar\omega_l \gtrsim B$), the $n>1$ bands play a more important role in the intermediate state sum when $h\nu$ is close to the threshold ($E_{x1}-\hbar\omega_l$), since then the $n=1$ energy denominator is not small compared to those for $n>1$.

The sum over intermediate states has been evaluated in two ways. In the first, the sum is rewritten as

$$\sum_n \frac{\varphi_n(0)[n|U|1]}{E_{xn}-h\nu}=\sum_{n=}^{N} \frac{\varphi_n(0)[n|U|1]}{E_{xn}-h\nu} + (\sum_n - \sum_{n=1}^{N}) \frac{\varphi_n(0)[n|U|1]}{E_{xn}-h\nu} \quad (15)$$

so as to separate out a small finite number N of terms which are to be evaluated exactly. To approximately evaluate the remaining terms on the right-hand side, which is the sum over all states with $n>N$, we replace E_{xn} in them by an "average excitation" $\langle E_{xn}\rangle$. The infinite summation, which is re-expressed as the sum over the whole spectrum minus the finite sum as indicated, can be carried out directly using the completeness property $\Sigma_n \varphi_n(0)\varphi_n(\mathbf{r})=\delta(\mathbf{r})$. The sum over the whole spectrum equals zero because the interaction vanishes at $\mathbf{r}=0$. With this result, the absorption coefficient can be shown to be

$$\alpha_{n'=1}(h\nu)\approx\alpha_1(h\nu)\left[\frac{\langle E_{xn}\rangle-E_{x1}}{\langle E_{xn}\rangle-h\nu}\right]^2 \times\left|\sum_{n=1}^{N} n^{-3/2}\left(\frac{E_{x1}-h\nu}{E_{xn}-h\nu}\right)\left(\frac{\langle E_{xn}\rangle-E_{xn}}{\langle E_{xn}\rangle-E_{x1}}\right) \times\frac{[n,0|U(\mathbf{q})|1]}{[1|U(\mathbf{q})|1]}\right|^2_{\mathbf{q}=\mathbf{q}_1}. \quad (16)$$

In principle, $\langle E_{xn}\rangle$ is a function of $h\nu$; but since $\langle E_{xn}\rangle-h\nu$ must be fairly large (i.e., $>B$) because of the subtracting out of the lower N bands and the contribution of the continuum, we can conveniently neglect this dependence. Numerical evaluation (see below) demonstrates that for a fixed $\langle E_{xn}\rangle$ the terms with $n\geq 2$ or 3 contribute only negligibly to the sum in (16).

In the other approach we explicitly calculate the matrix elements in a form which permits the summations to be carried out. The basis of this approach is the well-known fact that the bound-state and low-lying unbound-state radial functions for a given l (but varying principal quantum number) have rather similar r dependence (but different normalization) within the first few nodes, the region important for the evaluation of the matrix element. The mathematical expression of this[22] is the expansion of the (unnormalized) radial function for the discrete states in powers of n^{-2}:

$$r^{1/2}R_{nl}(r)=J_{2l+1}(z)+n^{-2}[\tfrac{1}{4}(l+1)(z/2)J_{2l+3}(z) -\tfrac{1}{12}(z/2)^2J_{2l+4}(z)]+O(n^{-4}), \quad (17)$$

where $z=(8r)^{1/2}$. For the continuum states $-n^{-2}$ is replaced by $(ka)^2=(\hbar^2k^2/2\mu)B^{-1}$. Since the expansion in that case is convergent only for the kinetic energy (of relative motion) small compared to B, it cannot be used in the sum over the whole continuum. With the n dependence separated out as in Eq. (17), the summation over the discrete spectrum can readily be carried out. In the computations below, the matrix elements for the $n=1$, 2, and 3 bands have been evaluated exactly and the others using (17) have been calculated with the neglect of terms $O(n^{-4})$.

Using $\int_0^\infty e^{-\gamma x}x^{\kappa/2}J_\kappa(2\sqrt{x})dx=\gamma^{-\kappa-1}\exp(-\gamma^{-1})$,[23] we find that

$$[n,l=0|U|n=1] =\{S_1(p_h)+n^{-2}[\tfrac{1}{4}S_3(p_h)-\tfrac{1}{12}S_4(p_h)]\} -\{p_h\rightarrow p_e\}, \quad (18)$$

where

$$S_\kappa(p)=-p^{-1}2^{\kappa+1}(1+p^2)^{-\kappa-1}\exp[-2/(1+p^2)] \times\{\sin[2p/(1+p^2)]\,\mathrm{Re}(1-ip)^{\kappa+1} +\cos[2p/(1+p^2)]\,\mathrm{Im}(1-ip)^{\kappa+1}\},$$

with Re and Im denoting, respectively, the real and imaginary parts. With (18) and after the computation of some sums over n, $\alpha(h\nu)$ is obtained from (12).

B. Contribution of $n>1$ Final States

The contribution from the $n>1$ final states starts at $h\nu=E_{x2}$ and tends to increase with increasing $h\nu$. To compute the sum $\sum'_{n'>1}$ in Eq. (12), we employ the simple generalization to $n'>1$ of the approach leading to Eq. (16). We obtain

$$\alpha(h\nu)=\sum_{\mathbf{n}'}{}' F_{\mathbf{n}'}(h\nu)q_1/q_{n'}, \quad (19)$$

where $F_{\mathbf{n}}(h\nu)$ is the expression in (16) with $[n,0|U(q)|1]|_{q_1}$ replaced by $[n,0|U(q)|\mathbf{n}']|_{q_{n'}}$. The factor $q_1/q_{n'}$ appropriately corrects for the density-of-

[22] See, for example, F. Ham, Quart. J. Appl. Math. **15**, 31 (1957).
[23] W. Gröbner and N. Hofreiter, *Integral Tafel II. Teil* (Springer-Verlag, Vienna, 1958), 2nd ed., p. 198.

states term and for the q^{-2} factor in the square of the electron-phonon interaction [Eq. (5)].

In contrast to the intermediate states, final states with $l>0$ must be included since the interaction scatters into states of all angular momenta. While, in general, one would expect the contributions to drop off with increasing l, it turns out that the $l=0$ states (for $n>1$) do not dominate the sum. To obtain an indication of the relative importance of the final states with different l, we note that since the recoil momenta (in units of a^{-1}) involved are small (i.e., $qa\lesssim 1$), the l component of the interaction goes roughly as

$$\begin{aligned} &j_l(qrm_h/M)+(-1)^{l+1}j_l(qrm_e/M)\\ &\quad\sim \tfrac{1}{6}q^2r^2(m_h^2-m_e^2)M^{-2}, \qquad l=0;\\ &\quad\sim q^lr^l[m_h{}^l+(-1)^{l+1}m_e{}^l]M^{-l}/(2l+1)!!, \quad l\neq 0. \end{aligned} \tag{20}$$

This suggests that the $l=1$ terms will be the largest contributors and that the $l\geqslant 3$ terms will be negligible for our purposes.

To evaluate the required matrix elements and sums over states we used the approach involving the expansion of R_{nl} in terms of n^{-2}. However, due to increasing complexity of the matrix elements with increasing l using Eq. (17), we have resorted to a somewhat modified approach based on the same general principle. Here we express $R_{nl}(r)$ within the first few nodes in terms of a few suitably chosen radial functions of moderately low principal quantum numbers. It can be readily demonstrated that for the radial functions normalized as $R_{nl}\to r^l/(2l+1)!$ for $r\to 0$,

$$\begin{aligned} R_{n,l}(r)=R_{\bar{n},l}(r)+(n^{-2}-\bar{n}^{-2})\bar{n}^2(\bar{n}-1)^{-2}(1-2\bar{n})\\ \times[R_{\bar{n},l}-R_{\bar{n}-1,l}]+O(\bar{n}^{-4}). \end{aligned} \tag{21}$$

As before, when $-n^{-2}$ is replaced by $(ka)^2$, the expansion is valid for the low-energy continuum states [i.e., $(ka)^2\ll 1$]. For the photon energies of interest the cutoff in the continuum states is at the worst at $ka<1$. Furthermore, since the squares of all the scattering matrix elements decrease fairly rapidly with decreasing recoil momenta, the contribution of the states with $(ka)^2\lesssim 1$ to the sum (integral) over states will be quite small and the use of (21) does not lead to an appreciable error.

In evaluating the sum (19) for CdTe, we have computed the contribution of the $n\leq 4$ bands separately. For the discrete bands with $n\geq 5$ we set $q_n=\bar{q}$ which was evaluated for $\bar{n}^{-2}=0.02$, a procedure introducing an error in these terms of the order of 2%, so that the sums could be carried simply. The integrals over the continuum states are carried out numerically. To avoid a considerable increase in the complexity of the computations, we have employed the relatively simple expression for $F_{n'}$ which corresponds to taking $N=1$ in Eq. (16). As we will see below, the contributions of the higher terms in Eq. (16) are quite small at the higher energy end of the relevant energy range. This is related to the fact that as $h\nu\to E_{x1}$, the contribution of the $n=1$ intermediate state becomes increasingly important.

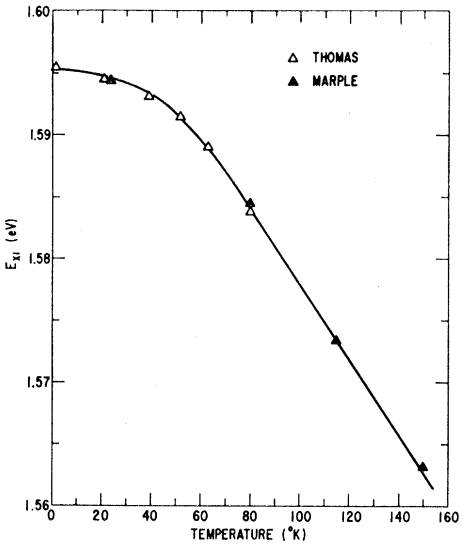

FIG. 2. The energy of the $n=1$ exciton line in CdTe as a function of temperature.

C. Application to CdTe

Fortunately, the parameters required to determine $\alpha(h\nu)$ are known with sufficient accuracy for CdTe to make a detailed comparison with experiment feasible. For the dielectric constants we will use $\epsilon_s=10.0$,[7,24] $\epsilon_\infty=7.05$,[25] and $\epsilon'=9.0$,[26] and for the phonon energy $\hbar\omega_l=0.0213$ eV.[27] Thomas's[28] reflectivity measurements have given $E_{x1}(T)$ from low temperatures up to about 80°K while recent work[12] has extended this up to 150°K. Figure 2 presents these results. Interpretations of the electrical[7] and Faraday rotation[29] studies have indicated an isotropic electron mass of magnitude $m_e=0.11\pm 0.01$.[29] The mass isotropy was confirmed by cyclotron resonance studies which yielded the mass value of $m_e=0.096\pm 0.005$.[8] The oscillator strength f_1, which determines the magnitude of α, has been obtained from a Kramers-Kronig analysis of reflectivity data. The value of $f_1=6.1\times 10^{-4}\pm 20\%$, or correspondingly $4\pi\beta_1=4.8\times 10^{-3}\pm 20\%$.[13] Of all the parameters, the hole mass m_h is the least well known. On the basis of the separation of the peaks in ϵ_2 due to $n=1$ and $n=2$

[24] A recent determination by D. T. F. Marple and S. Roberts (to be published) yields the value of $\epsilon_s=9.7$ at $T=4$°K. Berlincourt *et al.*, Ref. 37, obtained the value 9.65 at $T=90$°K.

[25] This value was obtained by extrapolating the room-temperature result [D. T. F. Marple, J. Appl. Phys. **35**, 539 (1964)] and the $T=90$°K result (D. T. F. Marple, unpublished) to low temperatures.

[26] D. T. F. Marple and H. Ehrenreich, Phys. Rev. Letters **8**, 87 (1962).

[27] R. E. Halsted, M. R. Lorenz, and B. Segall, J. Phys. Chem. Solids **22**, 109 (1961).

[28] D. G. Thomas, J. Appl. Phys. **32S**, 2298 (1961).

[29] D. T. F. Marple, Phys. Rev. **129**, 2466 (1963).

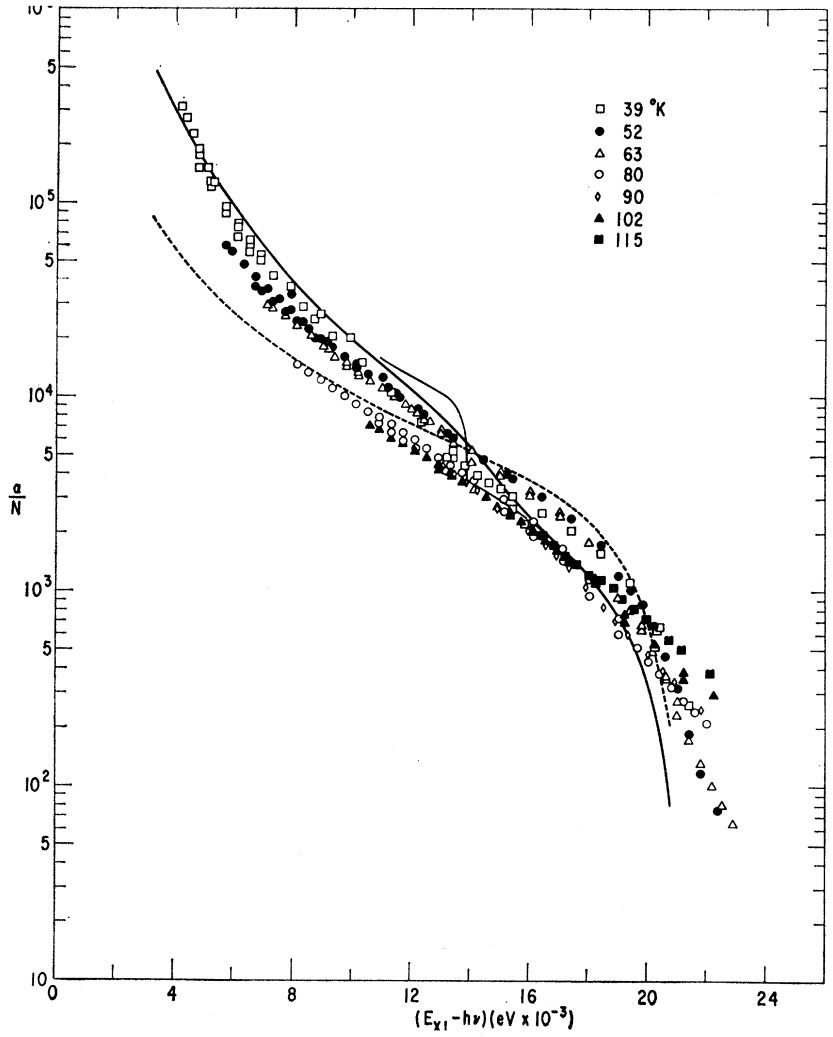

FIG. 3. A comparison of data from I and theory in the one-phonon region (i.e., $E_{x1}-h\nu<\hbar\omega_l$). According to Eq. (12), the plot should be essentially temperature-independent. The dashed curve represents the approximation, Eq. (14), in which only the contribution of the $n=1$ intermediate- and final-state exciton band is included, while the solid curve gives the results which include the contributions from the $n>1$ bands. For both cases the value $m_h=0.4$ has been used. The heavier solid curve includes the effect due to the broadening of the $n\geq 2$ levels. The finer segment around $E_{x1}-h\nu\approx 14$ meV represents the results for the unbroadened exciton spectrum (see Fig. 5 and the text).

excitons, derived from the reflection measurements,[13] the rough limits $0.25<m_h<0.5$ can be determined.[30] The absorption coefficient has been calculated for the three values $m_h=0.3$, 0.4, and 0.5.

In comparing the theory to the data in I, it is convenient to plot α/N against $E_{x1}(T)-h\nu$[8] in the one-phonon region since according to the theory this should remove the principal temperature dependences. (At low T only relatively small residual temperature effects would be expected. These would be attributable, for example, to the variation of linewidth (see Sec. IV) and some parameters (e.g., ϵ_s) with temperature.) This is borne out in Fig. 3, which shows data from I taken at a range of temperatures plotted in this fashion. The values of $\alpha(h\nu)$ employed in Fig. 3 were obtained by subtracting from $\alpha(h\nu)$ for a given temperature the measured 2°K absorption at $h\nu+E_{x1}(T)-E_{x1}(2°\text{K})$. The reason for this is, as suggested in I, that the absorption for $T\lesssim 24°$K appears to be an extrinsic effect. This is supported by the fact that for these temperatures $\alpha(h\nu)$ shifts rigidly with $E_{x1}(T)$. The dashed curve represents $\alpha_1(h\nu)N^{-1}$ (Eq. 14) for the parameters discussed above and $m_h=0.4$. It is apparent that the calculated curve qualitatively represents the data well; and this indicates that the mechanism employed is probably the correct one. However, quantitative discrepancies do exist. For example, near the threshold (e.g., at $E_{x1}-h\nu\approx 15$ to 19 meV), the data fall below the calculated curve by nearly a factor of two (this is most convincingly seen at moderately low temperatures where the two-phonon contributions, etc., are not so significant). At higher $h\nu$, the data lie well above this approximation with the discrepancy being greater than a factor of five at $E_{x1}-h\nu=4$ meV. The corresponding results for $m_h=0.5$ lie somewhat higher but do not provide a more satisfactory fit to the data. The $\alpha_1(h\nu)$ values for $m_h=0.3$

[30] The "light" and "heavy" hole (of the degenerate valence band) may be contributing to the broadening of the $n=2$ peak. But, for the consideration of this report the "heavy" hole is probably the more important one because of the larger density-of-states factor.

fall well below those for $m_h=0.4$ and are thus in even poorer agreement with the data.

In Fig. 4 we show the contribution of the various corrections discussed above for a $m_h=0.4$. The result obtained by summing over the discrete intermediate states, which is indicated by the dashed curve, is significantly below α_1 for $(E_{x1}-h\nu)$ between $\frac{1}{2}\hbar\omega_l$ and $\hbar\omega_l$. This indicates that there is some cancellation of the matrix element for $n=1$ by those of the higher intermediate bands. This is in line with the fact that the simplest application of the approximation involving the closure property leads to a complete vanishing of the sum {i.e., if E_{xn} is replaced by $\langle E_{xn}\rangle$ in the left-hand side of (15), we find $\sum_n(\langle E\rangle-h\nu)^{-1}\varphi_n(0)[n|U|1]=0$}. The results obtained using Eq. (16) with $N=3$ are shown for $\langle E_{xn}\rangle-E_{x1}=4.3B$, $7.5B$, and $10.7B$. For a fixed $\langle E_{xn}\rangle$, Eq. (16) converges fairly rapidly with the $n=3$ term being typically about 7% of the first term at the threshold end and dropping to a negligible value at the higher end of the range. The shape of the curve for the lowest value of $\langle E_{xn}\rangle-E_{x1}$ is too steeply rising and featureless, and in addition requires a somewhat too large value of f to obtain the correct magnitude. The curves for $7.5B$ and $10.7B$ are reasonably satisfactory in regard to both shape and magnitude considering the anticipated raising of the high-energy end by the final-state corrections. These values of $\langle E_{xn}\rangle$ are not unreasonable in view of the subtracting out of the $n=1$, 2, and 3 bands and the expected contribution of the continuum states. Also, we should note that the results are not very sensitive to the choice of $\langle E_{xn}\rangle$.

The correction arising from the $n>1$ final-state exciton bands, shown in Fig. 4(b), is clearly quite significant. It has a much larger magnitude than the corrections associated with the $n>1$ intermediate states

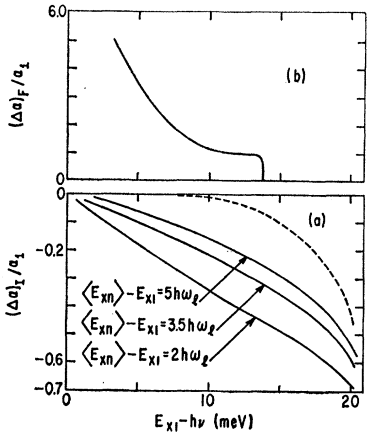

FIG. 4. Calculated contributions to the absorption coefficient from $n>1$ exciton bands. (a) The corrections to α_1 which arise from $n>1$ intermediate states. The dashed curve is the result obtained by including only the discrete spectrum while the solid curves are results obtained by Eq. (16) using the indicated value of the parameter $\langle E_{xn}\rangle$. (b) The contributions arising from the $n>1$ final-state bands. The value $m_h=0.4$ was used to obtain (a) and (b).

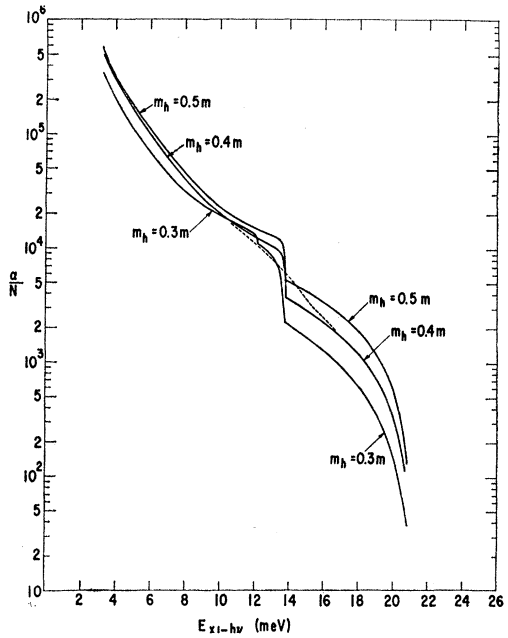

FIG. 5. The calculated values of $\alpha(h\nu)/N(\hbar\omega)$ for the hole masses $m_h=0.3$, 0.4, and 0.5. The dashed segment of the $m_h=0.4$ curve illustrates the effect of including the line broadening of the $n>1$ exciton states.

for $h\nu$ above the $n=2$ threshold. This correction is roughly four times as large as the simple approximate result, $\alpha_1(h\nu)$ [Eq. (14)], at the upper end of the experimental energy range (i.e., $E_{x1}-h\nu\approx 4$ meV). In line with our expectations, the $l=1$ final states contribute over 80% to the total while that for the $l=3$ states is at most about 1% (and that at the highest energy considered). For $h\nu$ only slightly greater than the threshold for the continuum states (i.e., $h\nu>E_G-\hbar\omega_l$) these states make the principal contribution to the sum. The sharp rise around $E_{x1}-h\nu\approx 14$ meV followed by a plateau is due to the fact that the $n=2$ $l=1$ contribution rapidly attains its peak value and then begins to drop off for $h\nu$ above the threshold for the $n=3$ and the higher discrete bands.

It is clear from the above that except when B is considerably larger than $\hbar\omega_l$, it is necessary to take into account the $n>1$ bands in order to obtain quantitatively significant results. For CdTe the contributions from these states are such as to reduce the absorption coefficient by roughly a factor of 2 near the one-phonon threshold and to raise it by about a factor of 5 at the highest observed values of α/N.

Figure 5 shows the sum of the various contributions to $\alpha(h\nu)/N$ in the one-phonon case for the masses $m_h=0.3$, 0.4, and 0.5. The curves for the different masses differ most for $h\nu$ below the $n=2$ threshold. The reason for this is that for the $n=1$ final state (and, in fact, for all states with even l), the electron and hole parts of the scattering matrix element cancel as $m_h/m_e\rightarrow 1$. For the $l=1$ states, on the other hand, the

matrix elements tend to increase as the mass ratio approaches unity. One feature of these curves which is clearly not evident in the data (Fig. 3) is the shoulder at $E_{x1}-h\nu\approx 0.014$ eV associated with the $n=2$ threshold. That this shoulder is not observed results from the appreciable line broadening for $n=2$ and higher exciton states at the relevant temperatures ($T\geq 40°$K). From the fact that structure in the 2°K reflectivity data which is attributed to the $n=2$ line is completely absent at 22°K,[13] we can infer that the $n=2$ linewidth is several meV at 20°K. If a linewidth of this magnitude had been incorporated in the calculation, the shoulder would be completely smoothed out. This is illustrated for the $m_h=0.4$ curve by the dashed segment which was obtained by the simple and admittedly crude procedure of folding the above result, Fig. 5, into a Lorenztian line shape function with a width $\Gamma=2$ meV.

Of the three curves in Fig. 5, the one for $m_h=0.4$ provides the best fit of the data. This curve, including the effect of the $n=2$ broadening, is shown as the solid curve in Fig. 3. It can be seen that except in the immediate vicinity of the one-phonon threshold the calculated result for $m_h=0.4$ is in good accord with the data over its full range (over which α/N varies by about 10^3). The discrepancies at the one-phonon threshold are most noticeable for $T\geq 80°$K and tend to increase with temperature. These are due primarily to the broadening of the $n=1$ line and to the contribution from the two-phonon process, both of which will be discussed below. The results for $m_h=0.5$ are a little too large for $h\nu<E_{x2}-\hbar\omega_l$ while the $m_h=0.3$ results are definitely too low in this region.

III. THE TWO-PHONON PROCESS

The process that we are concerned with here is a direct extension of that treated in Sec. II, and is schematically described in Fig. 1(b). In the first step of the third-order perturbation process, the crystal is excited from its ground state to an intermediate state consisting of an exciton in band n with $\mathbf{K}\approx 0$ (i.e., $|n;K=0\rangle$) by the annihilation of the photon. The exciton is then scattered into the second intermediate state $|n',\ \mathbf{K}=\mathbf{q}\rangle$ by the absorption of the phonon of wave vector $\mathbf{q}$; subsequently, it is scattered into the final state $|n'',\ \mathbf{K}=\mathbf{q}+\mathbf{q}'\rangle$ by the absorption of the phonon $\mathbf{q}'$. In the other possible set of intermediate states the order in which the phonons are absorbed is reversed.

The transition rate for this process is

$$w_{\mathbf{q},\mathbf{q}'}{}^{(n)}=\frac{2\pi e^2\eta(\kappa)|\xi_\kappa\cdot\mathbf{P}_{vc}|^2N(\hbar\omega)^2}{\epsilon' m^2\nu}u^2(\mathbf{q})u^2(\mathbf{q}')\left|\sum_{n',n''}\frac{\varphi_{n'}(0)}{E_{xn'}-h\nu}\left\{\frac{[\mathbf{n}'|U(\mathbf{q})|\mathbf{n}''][\mathbf{n}''|U(\mathbf{q}')|\mathbf{n}]}{E_{xn''}+\frac{1}{2}\hbar^2\mathbf{q}^2M^{-1}-h\nu-\hbar\omega_l}+(\mathbf{q}\rightarrow\mathbf{q}')\right\}\right|^2$$
$$\times\delta[E_{xn}+\tfrac{1}{2}\hbar^2(\mathbf{q}+\mathbf{q}')^2M^{-1}-h\nu-2\hbar\omega_l], \quad (22)$$

where $(\mathbf{q}\rightarrow\mathbf{q}')$ corresponds to the previous terms with $\mathbf{q}$ and $\mathbf{q}'$ interchanged.

This transition rate and the related absorption coefficient are considerably more difficult to compute than the corresponding one-phonon quantities and, consequently, we will not attempt quite as detailed an analysis. We consider the quantity inside the absolute sign in (22), which is the analog of (15), and carry out the sums over the two sets of intermediate states using the approach employing the closure property. (However, to avoid excessive complexity, only the $n=1$ band is subtracted out of both sums.) When the sums are carried out successively, we obtain

$$M_2(\mathbf{q}\mathbf{q}')=\frac{\varphi_1(0)}{E_{x1}-h\nu}\left(\frac{\langle E_{xn'}\rangle-E_{x1}}{\langle E_{xn'}\rangle-h\nu}\right)\left\{[1|U(\mathbf{q})|1][1|U(\mathbf{q}')|\mathbf{n}]\right.$$
$$\times\left[\frac{1}{E_{x1}+\frac{1}{2}\hbar^2\mathbf{q}^2M^{-1}-\hbar\omega_l-h\nu}-\frac{1}{\langle E_{xn''}\rangle+\frac{1}{2}\hbar^2\mathbf{q}^2M^{-1}-\hbar\omega_l-h\nu}\right]$$
$$\left.+\frac{[1|U(\mathbf{q})U(\mathbf{q}')|\mathbf{n}]}{\langle E_{xn''}\rangle+\frac{1}{2}\hbar^2\mathbf{q}^2M^{-1}-\hbar\omega_l-h\nu}+(\mathbf{q}\rightarrow\mathbf{q}')\right\}, \quad (23)$$

where $(\mathbf{q}\rightarrow\mathbf{q}')$ indicates the previous terms with $\mathbf{q}$ and $\mathbf{q}'$ interchanged. In principle, the two quantities $\langle E_{xn'}\rangle$ and $\langle E_{xn''}\rangle$ which arise from the two factors in the original energy denominator are different, but because the difference should be small and because keeping them different would essentially introduce an extra adjustable parameter, we will in general set both of them equal except when we consider the final-state corrections (for $h\nu\rightarrow E_{x1}-\hbar\omega_l$) below. We will take this parameter to have a value ($7.5B$) which provided reasonable results for the one-phonon case.

To calculate the absorption coefficient from (22), it is necessary to sum over all phonon wave vectors $\mathbf{q}$ and $\mathbf{q}'$ and all final bands n. Converting the sums to integrals over the $\mathbf{q}$'s in the standard way, and carrying out the angular integrals (most simply accomplished by choosing the polar axis to be along one of the two vectors, say, $\mathbf{q}$), we

obtain

$$\sum_{\mathbf{qq}'}|M_2(\mathbf{qq}')|^2=(2M/\hbar^2)[V^2/(2\pi)^4]\left[\frac{\varphi_1(0)}{E_{x1}-h\nu}\right]^2\left(\frac{\langle E_{xn}\rangle-E_{x1}}{\langle E_{xn}\rangle-h\nu}\right)^2\int_0^\infty q\,dq\int_{|x_n-q|}^{(x_n+q)}q'dq'|\{\ \}'|^2, \tag{24}$$

where $x_n^2=2M\hbar^{-2}(h\nu+2\hbar\omega_l-E_{xn})$ and $\{\ \}'$ is the bracket in Eq. (23) with the restriction that $2\mathbf{q}\cdot\mathbf{q}'=x_n^2-\mathbf{q}^2-\mathbf{q}'^2$. Using (11), (22), and (24) and setting $q=2za^{-1}$, we obtain finally for the two-phonon part of the absorption constant

$$\alpha_{2\,\mathrm{ph}}=\frac{\epsilon_s}{\pi a}\frac{4\pi\beta}{(\epsilon')^{1/2}}\left(\frac{e^2}{\hbar c}\right)\left(\frac{M}{4\mu}\right)^3\left(\frac{\hbar\omega_l}{B}\right)^2(\epsilon_\infty^{-1}-\epsilon_s^{-1})^2\left(\frac{E_{x1}}{E_{x1}-h\nu}\right)^2\left(\frac{\langle E_{xn'}\rangle-E_{x1}}{\langle E_{xn'}\rangle-h\nu}\right)^2N^2(\hbar\omega)\sum_n I_n(h\nu), \tag{25}$$

where

$$I_n(h\nu)=\int_0^\infty\frac{dz}{z}\int_{|\beta_n-z|}^{\beta_n+z}\frac{dz'}{z'}|[1|U(2za^{-1})|1][1|U(2z'a^{-1}|\mathbf{n}][(b+z^2)^{-1}-(d+z^2)^{-1}]$$
$$+(d+z^2)^{-1}[1|U(2za^{-1})U(2z'a^{-1})|\mathbf{n}]+(z\to z')|^2,$$

with

$$b=(E_{x1}-\hbar\omega_l-h\nu)M/4\mu B,$$
$$d=(\langle E_{xn''}\rangle-\hbar\omega_l-h\nu)M/4\mu B,$$

and

$$\beta_n=\tfrac{1}{2}x_na.$$

For $h\nu<E_{x1}+\frac{3}{4}B-2\hbar\omega_l$, the $n=2$ threshold, only $I_{n=1}\neq0$. As in the one-phonon case, for photon energies at which the final-state corrections become significant the lowest exciton band begins to dominate in the second set of intermediate states (n'') by virtue of the relative smallness of the corresponding energy denominator. Thus, in computing the final-state corrections we restrict n'' to $n''=1$, or equivalently we set $\langle E_{xn''}\rangle=\infty$ in (23). To evaluate the I_n for the high discrete states or continuum states, we approximate the matrix elements $[1|U|n]$ by the technique discussed in Sec. II.

We note that the expression for the two-phonon part of the absorption constant above is only valid for $E_{x1}-h\nu>\hbar\omega_l$ because of a singularity due to the vanishing of the second energy denominator for $h\nu$ greater than the one-phonon threshold. This singularity is eliminated when the exciton linewidth is properly incorporated into the theory.

A. Comparison with Experiment

Since the theory predicts that the absorption constant is essentially proportional to $N(\hbar\omega_l)^2$ in the two-phonon region, it is convenient to plot αN^{-2} against $E_{x1}(T)-h\nu$. From the absorption-constant measurements of I at 90, 102, 115, 130, and 150°K and $E_{x1}(T)$ from Fig. 2, we obtain Fig. 5. It is evident that within the experimental uncertainties [e.g., $E_{x1}(T)$ is not known to be better than ±0.001 eV at 150°K], the data thus plotted form a curve that is essentially independent of temperature. This in itself is some confirmation of the theory.

The solid curve in Fig. 6 represents the calculated values of $\alpha(h\nu)N^{-2}$ in the two-phonon region evaluated with the same parameters employed to obtain the one-phonon results depicted in Fig. 4 (in particular, $m_h=0.4$). For comparison, the results for $m_h=0.5$ are shown as the dashed curve. At the higher energy end of the range considered, the calculations include the final-state contributions from $n>1$ estimated in the manner indicated above. The calculated results for $m_h=0.4$ (the parameter yielding the best fit for the one-

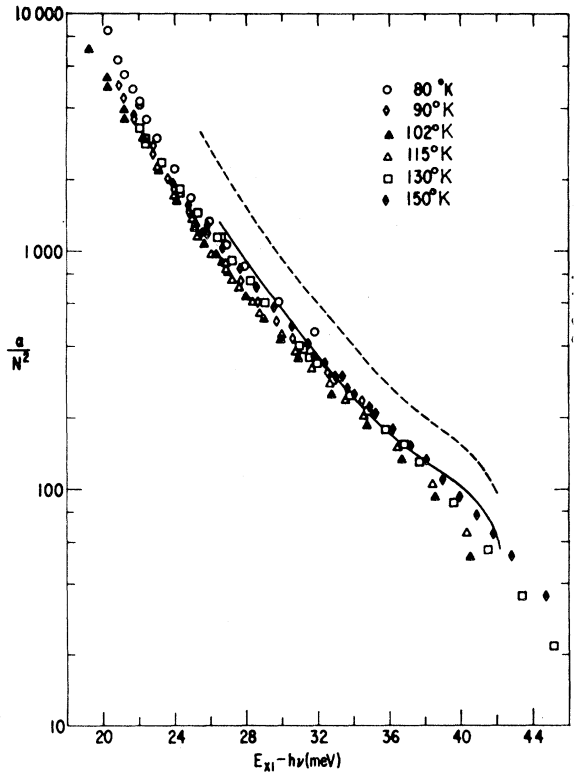

FIG. 6. A comparison of the data and theory in the two-phonon region. The plots are in a form analogous to that used in Fig. 3. The solid curve represents the calculated result for $m_h=0.4$ while the dashed curve that for $m_h=0.5$.

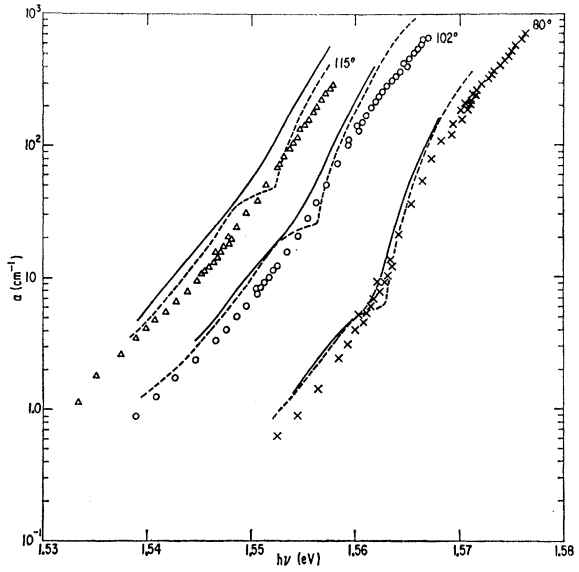

FIG. 7. Approximate treatment of the effect of exciton line broadening on α in the one-phonon threshold region. The dashed curves are the sums $\alpha_{1\,\mathrm{ph}}+\alpha_{2\,\mathrm{ph}}$ calculated for zero linewidth. The solid curves are the results of folding the above into Gaussian line-shape functions with widths obtained from reflectivity data given in Ref. 12.

phonon case) are seen to be in quite good agreement with the data in regard to both magnitude and shape. In fact, considering the rather approximate nature of our evaluation of (22), the agreement is as satisfactory as one has reason to expect. The small discrepancies around the two-phonon threshold ($E_{x1}-h\nu\approx 2\hbar\omega_l\approx 42.6$ meV) are analogous to those at the one-phonon threshold, and are due to the considerable linewidth at the temperatures of interest and to the three-phonon contributions. The results for $m_h=0.5$ are too high by almost a factor of 2 for $E_{x1}-h\nu$ in the range 26 to 30 meV. This tends to strengthen our belief that $m_h=0.4$ is the more appropriate (average) value for the hole mass.

IV. THE ABSORPTION COEFFICIENT AT MODERATELY HIGH TEMPERATURES

In this section we consider some aspects of the absorption at moderately high temperatures. The sum at different temperatures of the one- and two-phonon contributions to α calculated above must exhibit distinct thresholds. These thresholds are quite evident in the data (I, Fig. 2) for the $T\lesssim 80$°K, but are blurred out at higher temperatures. This smoothing out of the threshold shapes is due to the combined effect of the relative increase of the two-phonon contribution and the increase of the exciton line breadth with increasing temperature. To illustrate this, we employ the simple and crude procedure of folding the sum of $\alpha_{1\,\mathrm{ph}}$ and $\alpha_{2\,\mathrm{ph}}$ (extrapolated into the one-phonon region)[31] into a Gaussian line-shape function. The results obtained for $T=80°$, 102°, and 115°K using the approximate line widths of 3, 5, and 7 meV, respectively, obtained from reflectivity measurements[12] are shown in Fig. 7. The similarity in shape to the data is sufficiently good to indicate the role of the exciton line broadening. The larger linewidth and the poor convergences of the perturbation series at higher temperatures make the above approach seem very dubious there. In a more complete treatment the level broadening (and level shift) would be more integrally incorporated in the calculation.

Another noteworthy feature of data in I (Fig. 2) is that α has a nearly exponential dependence on $E_{x1}-h\nu$ for $T\gtrsim 130$°K. This exponential dependence is an example of the well-known Urbach's rule, which has been the subject of considerable discussion.[17] Most of these discussions have taken the point of view that the Urbach behavior must be understood in terms of localized excitons, self-trapped in the case of intrinsic excitons. The strong-coupling configurational coordinate approach has been invoked (even though weak coupling might be appropriate for the exciton line region) and the absorption is pictured as being accompanied by the absorption of many phonons. Toyozawa[32] has shown that in this framework Urbach-rule behavior follows from the existence of local normal modes for which the linear term in the electron-phonon interaction vanishes.

The success of the present weak-coupling perturbation calculations tends to argue against the necessity of the above picture for the case of intrinsic excitons, at least, in the compound semiconductors. While it is true that our results become unreliable at the temperatures at which the fully developed Urbach dependence occurs, they are reliable and are in good agreement with the data at slightly lower temperatures at which α is approximately Urbachian. It is thus suggested that, at least in the partially polar materials like CdTe, Urbach's rule is initimately related to the mechanism considered in this paper—that of photon absorption through the creation of the (unlocalized) excitons accompanied by the annihilation of a few LO phonons. We have not obtained the analytical exponential expression from our results. This would require more complete treatment in which higher-order effects would be included. We note that during the period in which this paper was being written, Mahan[33] has calculated the spectral-density

[31] As noted earlier, $\alpha_{2\,\mathrm{ph}}$ is singular for $h\nu>E_{x1}-\hbar\omega_l$ when the linewidth is neglected. The extrapolation used was an extension of the solid curve in Fig. 6 to the value 2.8×10^3 at $E_{x1}-h\nu=\hbar\omega_l$. In principle the procedure used is inconsistent since the extrapolation of $\alpha_{2\,\mathrm{ph}}$ makes sense only when $\Gamma\neq 0$. However, for the purposes we are concerned with it is the smearing of the one-phonon edge into the (two-phonon) region of lower absorption that is most significant.

[32] Y. Toyozawa, Technical Reports of the Institute for Solid State Physics (Tokyo), Series A, No. 119, 1964 (unpublished).

[33] G. D. Mahan, Phys. Rev. 145, 602 (1966).

function for an electron coupled to LO phonons by Eqs. (4) and (5) in a certain intermediate-coupling scheme. He finds that for $kT/\hbar\omega_l \ll 1$ the spectral function has the Urbach energy dependence.

V. MECHANISMS INVOLVING OTHER ELECTRON-PHONON COUPLING

Although it has been shown in the previous sections that the absorption edge for CdTe can be understood quantitatively in terms of the process involving the polar interaction between the excitons and LO phonons, it is of interest to evaluate the role that other electron-phonon interactions play in the spectral region under consideration. Inasmuch as the data (see Fig. 3) suggest that some high-energy phonons, most probably optical modes, are involved over at least a major part of the energy range, we will start by considering couplings with the optical modes and in particular those around $\mathbf{q}=0$. It is well known that there is no coupling to the polarization of the pure transverse modes because $\mathrm{div}\mathbf{P}_t=0$. The electronic particles also couple to the optical modes of both polarizations through a nonpolar interaction which can be expressed by (4) if the function $u(q)$ for the hole, for example, is given by $u_{h\sigma}{}^2=2\hbar^2C_4{}^2/\rho V\hbar\omega_\sigma a_L{}^2$, where ρ is the density of the crystal, a_L is the lattice constant, and C_4 is a constant having the dimension of an energy.[34] We need only consider the interaction with the hole since the coupling with the electron is very much smaller.[35] By comparing the nonpolar to the polar interaction, Eq. (5), we find that the ratio of the corresponding absorption constants for the one-phonon case is approximately $C_4{}^2(qa)^2[\pi\rho(\omega e a_L a)^2\times(\epsilon_\infty{}^{-1}-\epsilon_s{}^{-1})]^{-1}$, where $(qa)^2$ is evaluated for a typical recoil. From energy conservation it is found typically $(qa)^2\lesssim 10$. For CdTe, then, the ratio is no more than $3\times10^{-4}C_4{}^2(\mathrm{eV})$, and thus is very small for any reasonable value of C_4 (which is thought to be about 10 eV).[34,36]

The contribution from interactions with phonons having wave vectors far removed from the center of the zone (i.e., $q\sim 2\pi/a_L$), can be seen to be unimportant even at critical points where the phonon density is relatively large. This follows from the magnitude of the square of the matrix element of $u(\mathbf{q})$ which is roughly $[1+(\pi m_e a/Ma_L)^2]^{-4}$ and is typically in the range 10^{-2} to 10^{-4}, and from the fact that the coupling constant would be smaller than that for the polar interaction at $\mathbf{q}=0$.

For the two-phonon region, we must consider in addition to the above the possible role of electron-phonon coupling terms quadratic in the lattice displacements. With these terms the annihilation of the two phonons would take place in one step (a second-order perturbation for the complete process of photon and phonon absorption) in contrast to the two steps required in the case of the linear interactions. While at present very little is known about the magnitude of these terms, it seems unlikely that they would be of comparable importance to the iteration of the polar interaction. This view is based on the estimate of the relative importance of the polar and nonpolar interactions made above. One feature of the bilinear interaction that is noteworthy is that, in contrast to the one-phonon and iterated two-phonon cases, certain matrix elements, $(n|\exp[i(\mathbf{q}+\mathbf{q}')\cdot\mathbf{r}]|n')$ with $\mathbf{q}+\mathbf{q}'\approx 0$ and $n=n'$, are not small for $\mathbf{q}$ far from the center of the zone. Since, however, this can occur only in a restricted part of the available phase space (i.e., for $\mathbf{q}\approx-\mathbf{q}'$), and, since the effective coupling constant is probably not very large, the effect of these bilinear terms is small compared to that of the iterated polar interaction considered in Sec. III.

Finally, we consider the contribution of processes involving the absorption of acoustic phonons, which might conceivably be significant at $h\nu$ close to the $n=1$ exciton line particularly at low temperature. From conservation of momentum and energy it is found that $E_{x1}-h\nu=\hbar v_s q-\hbar^2q^2/2M$ for the one-phonon process, and that $E_{x1}-h\nu$ has a maximum value of $\frac{1}{2}Mv_s{}^2$, where v_s is the sound velocity. Using the typical value of 4×10^5 cm/sec for v_s, it is found that $(E_{x1}-h\nu)_{\max}\approx 5\times10^{-5}$ eV. Thus, while this process might contribute to the exciton "line" shape and width, it does not contribute to the absorption of interest in this paper. The smallness of $(E_{x1}-h\nu)_{\max}$ results from the fact that the exciton's recoil energy is larger than the phonon energy except for very small q, namely, $q<2Mv_s/\hbar$. For the two-phonon process, however, $E_{x1}-h\nu=\hbar v_s(q+q')-\hbar^2(\mathbf{q}+\mathbf{q}')^2/2M$, and the recoil energy is very small when $\mathbf{q}'\approx-\mathbf{q}$. In this case $E_{x1}-h\nu\approx 2\hbar v_s q$, values of which are in the range of interest for reasonably large q (i.e., $q\gtrsim 0.2K_{BZ}$).

The relative importance of the piezoelectric and deformation-potential couplings for the two-phonon case can be gauged by the ratio $[4\pi Ce/\epsilon_s E_1 q_i]^4$, where C is the piezoelectric constant, E_1 the deformation potential for the holes, and $q_i\approx(E_{x1}-h\nu)/2\hbar v_s$ is the minimum value of q. With the value of 2 eV for the presently poorly known value of E_1 and $C=1.01\times10^4$ (esu)/cm^2,[37] the ratio for CdTe is $\lesssim 10^{-3}$ for all $h\nu$ of interest. The ratio is smaller than unity for all other II–IV and III–V compounds except possibly for those few having much larger piezoelectric constants (e.g., CdS and ZnO).

From the remark made above about the matrix elements of the bilinear terms and the fact that $\mathbf{q}\approx-\mathbf{q}'$ for the two acoustic-phonon processes of interest, it is reasonable to question whether the bilinear terms in the interaction with acoustic phonons can be neglected. One means of obtaining some information about the magni-

[34] H. Ehrenreich and A. W. Overhauser, Phys. Rev. **104**, 331 (1956).

[35] The matrix element corresponding to C_4 vanishes for the Γ_1 Bloch state.

[36] M. Aven and B. Segall, Phys. Rev. **130**, 81 (1963).

[37] D. Berlincourt, H. Jaffe, and L. R. Shiozawa, Phys. Rev. **129**, 1009 (1963).

tude of this interaction, which can be written

$$D_{\mathbf{q},\mathbf{q}'}{}^{(j)}(a_{\mathbf{q}}a_{\mathbf{q}'}e^{i(\mathbf{q}+\mathbf{q}')\cdot\mathbf{r}_j}+a_{\mathbf{q}}{}^{*}a_{\mathbf{q}'}e^{i(\mathbf{q}'-\mathbf{q})\cdot\mathbf{r}})+\text{H.c.},$$

is to note that it leads to a shift of the band edge which in lowest order is

$$\Delta E_G\approx 2\hbar(\pi^2\rho v_s)^{-1}\int_0^{q_m} qdq\, N(\hbar\omega_q)[D_{qq}{}^{(e)}+D_{qq}{}^{(h)}].$$

If the $D_{q,q}$ are relatively slowly varying functions of q for q up to $q_T\approx kT/\hbar v_s$, the above is roughly $(3\rho\hbar v_s{}^3)^{-1}\times(\bar{D}^{(e)}+\bar{D}^{(h)})(kT)^2$, where $\bar{D}$ denotes the average of the D_{qq} over $0\leq q\leq q_T$. It is known empirically that the band edges of the compounds exhibit a shift proportional to T^2 from $T=0$ to $T\approx 100$°K (see Fig. 2). If the above expression for ΔE_G accounted for the observed shift, $\bar{D}a_L{}^2\approx 1$ eV. However, since Mahan[38] has shown that the band-edge shift can be reasonably well accounted for by the deformation-potential interaction alone, $\bar{D}$ is probably at most only a fraction of the above value. From these considerations we have estimated that the bilinear terms could not contribute to the absorption coefficient as much as the iterated-linear term. This proves to be sufficient for our present purposes. We note that a strong q dependence in the $D_{q,q}$ would lead to a temperature dependence different from the observed T^2 behavior. This fact implies a small magnitude for such terms.

We have estimated the absorption coefficient for the two acoustic-phonon process with the deformation potential interaction using Eq. (A2) of the Appendix and the parameters employed in Secs. II and III. For any reasonable value of the deformation potential (i.e., $E_1<10$ eV), the resultant absorption coefficient is too low by several powers of ten for all photon energies of interest (i.e., $E_{x1}-h\nu\geq 4$ meV).

It thus appears that no electron-phonon interaction other than the polar coupling to the LO phonons can contribute appreciably in the spectral region of interest (i.e., the range of the present data).

VI. CONCLUSIONS

It has been shown that the calculated optical-absorption coefficient corresponding to the mechanism of LO phonon-assisted "direct" exciton creation is in quantitative agreement with the absorption of CdTe in the edge region reported in I. The only essential adjustable parameter used in this calculation is the average hole mass which was taken to be 0.4 m, a value compatible with the observed exciton line spectrum. The agreement extends over a spectral region extending from just below $h\nu=E_{x1}$ down to $h\nu\approx E_{x1}-2\hbar\omega_l$ and over a considerable range of temperatures—from about 40°K up to about 150°K, where the simple perturbation employed probably ceases to be useful. On the basis of these results, other proposed mechanisms for the edge absorption, such as the one associated with the electric fields at the surface,[39] can be ruled out for this material.

Aside from providing an understanding of the absorption edge itself, these results coupled with the demonstration in I that the CdTe data cannot be understood in terms of an indirect band gap, as had been suggested[1] earlier, strongly indicate that the band gap in CdTe is direct and is located at $\mathbf{k}\approx 0$.

The present calculations have shown that the higher exciton bands (i.e., $n>1$ and the continuum) make very significant contributions to the absorption process considered. For CdTe, for example, it was found that through a cancellation of the matrix elements the higher intermediate states lead to an approximate halving of the absorption constant for photon energies just above the one-phonon threshold. On the other hand, the $n>1$ final-state bands yield appreciable positive contributions: at the highest energy at which data are available ($E_{x1}-h\nu=0.004$ eV), the present results are approximately five times larger than the simple result obtained by restricting the initial and final states to the $n=1$ band.[9,10] It is thus clear that, while the simple approximation leads to a qualitative understanding of the absorption, the corrections considered above must be included in a quantitative study.

From the agreement of the present calculations with the absorption data up to temperatures at which Urbach's behavior is manifested, it is concluded that the mechanism considered in this paper is the one underlying Urbach's rule in moderately polar materials like the II–VI semiconducting compounds and, perhaps, even in more polar materials. It was noted that the exciton linewidths at the relevant temperatures are sufficiently large to smooth out the distinctive spectral features (e.g., threshold edges) found at lower temperatures and in the calculations in which the widths are neglected. In the previous discussions of Urbach's rule, significant localization (i.e., self-trapping) appears to be required. In contrast to these approaches, which are essentially strong-coupling approaches and which employ a configuration coordinate model, the present mechanism retains the free (mobile) exciton and the (unlocalized) lattice phonons.

ACKNOWLEDGMENTS

The author wishes to thank D. T. F. Marple for many fruitful discussions. He also wishes to thank F. S. Ham and G. D. Mahan for helpful discussions. To Miss E. L. Kreiger goes his deep appreciation for her considerable assistance with the computations.

[38] G. D. Mahan, J. Phys. Chem. Solids **26**, 751 (1965).

[39] D. Redfield, Phys. Rev. **140**, A2056 (1965).

APPENDIX: CALCULATION OF $\alpha_{2ac}(h\nu)$

The approximate calculation of the absorption coefficient for the process involving the absorption of two acoustic phonons, $\alpha_{2ac}(h\nu)$, generally follows the procedures used in Secs. I and III. In particular, use is made of Eq. (22) with a $u(\mathbf{q})$ appropriate for coupling to acoustic modes and with $\hbar\omega_l$ replaced by $\hbar\omega(q)=\hbar vq$. For the deformation-potential interaction, the coupling we will consider (see Sec. V),

$$u_j(\mathbf{q})=E_j(\hbar/2\rho Vv)^{1/2}q^{1/2}, \tag{A1}$$

where E_j is the deformation potential for the electron ($j=e$) and hole ($j=h$). Since, as noted in Sec. V, we are concerned with photon energies such that $E_{x1}-h\nu\approx 3$ to 5 meV, we can reasonably use the approximation that only the $n'=1$ term of the first intermediate state summation need be retained. Performing the summation over the second set of intermediate states (n'') by the same procedure utilized in Sec. III, we obtain for the quantity analogous to $M_2(\mathbf{q},\mathbf{q}')$ a result identical to Eq. (23) except that the factor $(\langle E_{xn'}\rangle-E_{x1})/(\langle E_{xn''}\rangle-h\nu)$ is replaced by unity (and $\hbar\omega_l$ by $\hbar vq$ and $\hbar vq'$).

It can readily be seen that the creation of final-state excitons in a $n>1$ band requires rather energetic acoustic phonons and thus occurs with a much lower transition rate than for the $n=1$ band. The result can be legitimately simplified by requiring that $n=1$.

As noted in Sec. V, conservation of energy requires that $\mathbf{q}\approx-\mathbf{q}'$ for $h\nu$ in the range of interest. With this fact, the integral over $\mathbf{q}'$ can be performed and it is found after some manipulations that the result can be written as

$$\alpha_{2ac}(h\nu)\approx\frac{4\pi\beta}{(\epsilon')^{1/2}}\frac{E_h{}^4}{(2\pi)^3}\frac{\hbar c}{e^2}\frac{B\epsilon_s}{(\rho cv)^2}\times\left(\frac{2M}{\hbar^2}\right)^{7/2}\left(\frac{4\hbar v}{a}\right)^{1/2}\left(\frac{E_{x1}}{E_{x1}-h\nu}\right)^2 I_{ac}(h\nu,T),$$

$$I_{ac}(h\nu,T)=\int_{zi}^{\infty}dz\,n^2(z,T)(z-z_i)^{1/2}\times\{[g(p_e/2)+E_eE_h^{-1}g(p_h/2)]^2\times[[z^2-Az+d(h\nu)]^{-1}-[z^2-Az+\bar{d}(\nu)]^{-1}]+[1+(E_e/E_h)^2+2E_eE_h^{-1}g(z)][z^2-Az+\bar{d}(\nu)]^{-1}\}^2, \tag{A2}$$

with

$$g(z)=(1+z^2)^{-2},$$
$$d(\nu)=(E_{x1}-h\nu)M/4\mu B,$$
$$\bar{d}(\nu)=(\langle E_{xn''}\rangle-h\nu)M/4\mu B,$$
$$A=Mva/\hbar,$$
$$n(z,T)=[\exp(\gamma z/T)-1]^{-1},$$
$$z_i=(E_{x1}-h\nu)a/4\hbar v,$$
$$\gamma=2\hbar v/aK_B,$$
$$p_j=qam_j/M.$$